

Appendix A. Supplementary data

*Areej Merhi,^{a,b} Guillaume Grelaud,^{a,c} Nicolas Ripoche,^{a,c} Adam Barlow,^c Marie P. Cifuentes,^c Mark G. Humphrey,^{*c} Frédéric Paul^{*a} and Christine O. Paul-Roth^{*a}*

A Zinc(II) Tetraphenylporphyrin Peripherally Functionalized with Redox-Active “*trans*-[(η^5 -C₅H₅)Fe(η^5 -C₅H₄)C≡C](κ^2 -dppe)₂Ru(C≡C)-” Substituents: Linear Electrochromism and Third-Order Nonlinear Optics

Including:

- 1. Labelling Scheme in NMR Spectral Assignments and ¹³C NMR Spectrum** p. S2
- 2. Cyclic Voltammogram of 4** p. S4
- 3. ¹H NMR Spectrum of 2[PF₆]₄** p. S5
- 4. Spectroelectrochemistry of 3** p. S6
- 5. Z-scan Plots for 4** p. S7

1. Labelling Scheme in NMR Spectral Assignments and ^{13}C NMR Spectrum

$^{13}\text{C}\{^1\text{H}\}$ NMR (δ , 125 MHz, CD_2Cl_2): 150.6 (s, $\text{C}_{\alpha\text{-pyrrolic}}$), 137.7 (m, 2 $\text{C}_{\text{ipso/dppe}}$), 134.8 (m, 2 $\text{CH}_{\text{ortho/Ph/dppe}}$), 134.6 (s, $\text{CH}_{\text{Ar}}[\text{C}_b]$), 132.2 (s, $\text{C}_{\beta\text{-pyrrolic}}$), 130.1 (s, $\text{C}_{\text{Ar}}[\text{C}_d]$), 129.1 & 129.0 (s, $\text{CH}_{\text{para/Ph/dppe}}$), 128.5 (s, $\text{CH}_{\text{Ar}}[\text{C}_c]$), 127.5 & 127.3 (s, $\text{CH}_{\text{meta/Ph/dppe}}$), 123.0 (s, C_{meso}), 116.9 (s, $\text{RuC}\equiv\text{C}[\text{C}_e]$), 112.6 (s, $\text{RuC}\equiv\text{C}[\text{C}_h]$), 78.3 (s, $\text{C}_{\text{CpC}\equiv\text{C}}$), 70.2 (s, $\text{CH}_{\text{CpC}\equiv\text{C}}$), 70.0 (s, C_5H_5), 67.5 (s, $\text{CH}_{\text{CpC}\equiv\text{C}}$), 33.1 (m, CH_2/dppe); 2 $\text{RuC}\equiv\text{C}$ [$\text{C}_{\text{f-g}}$] and 1 $\text{C}_{\text{Ar}}[\text{C}_a]$ not observed, possibly overlapped. Proposed attribution based on HMBC and HMQC-type polarization transfer.

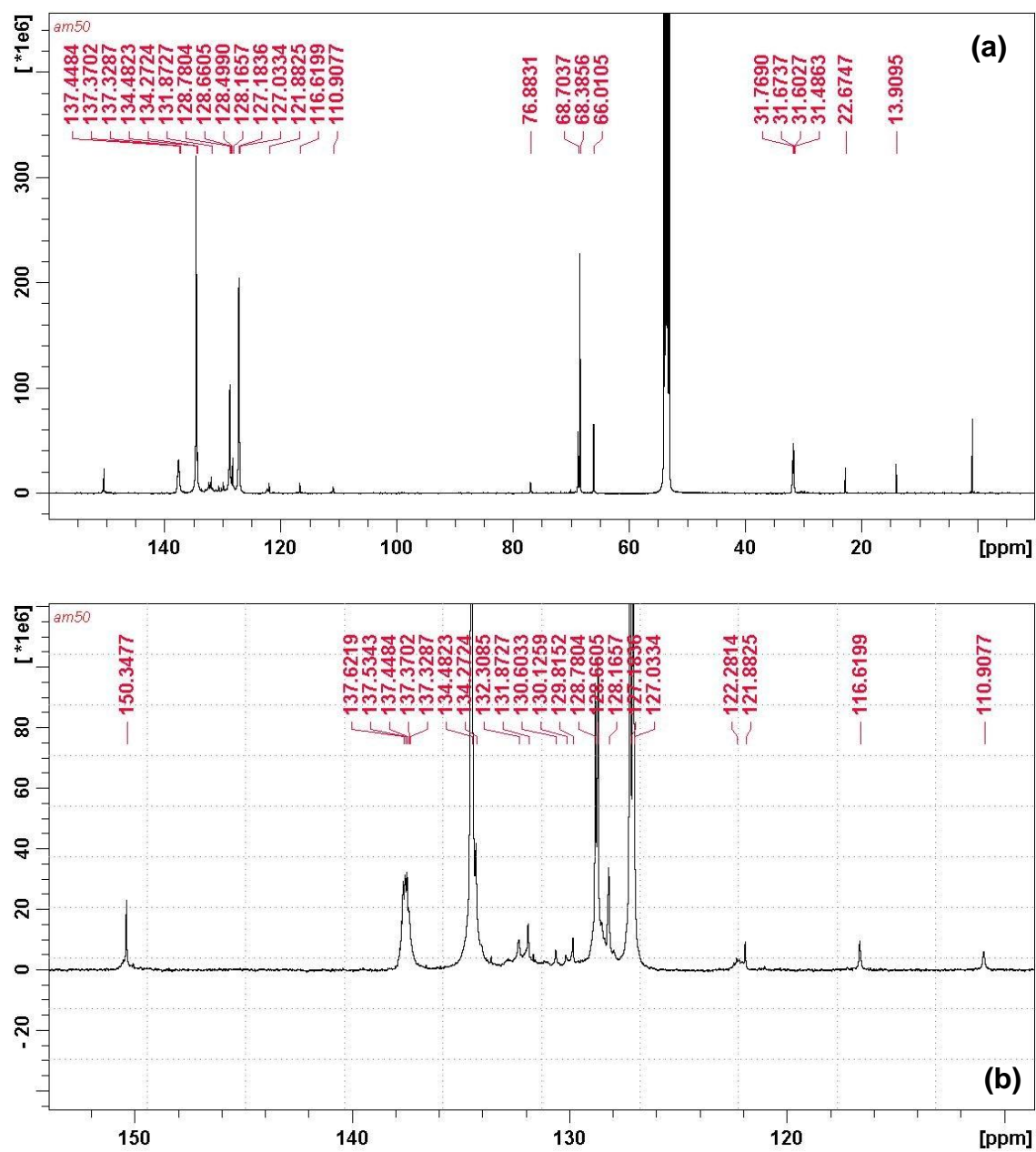


Fig. S1. (a) Full ^{13}C NMR spectrum of **4** in CD_2Cl_2 at 300 K. (b) Expanded part of spectrum (a).

2. Cyclic Voltammogram of 4

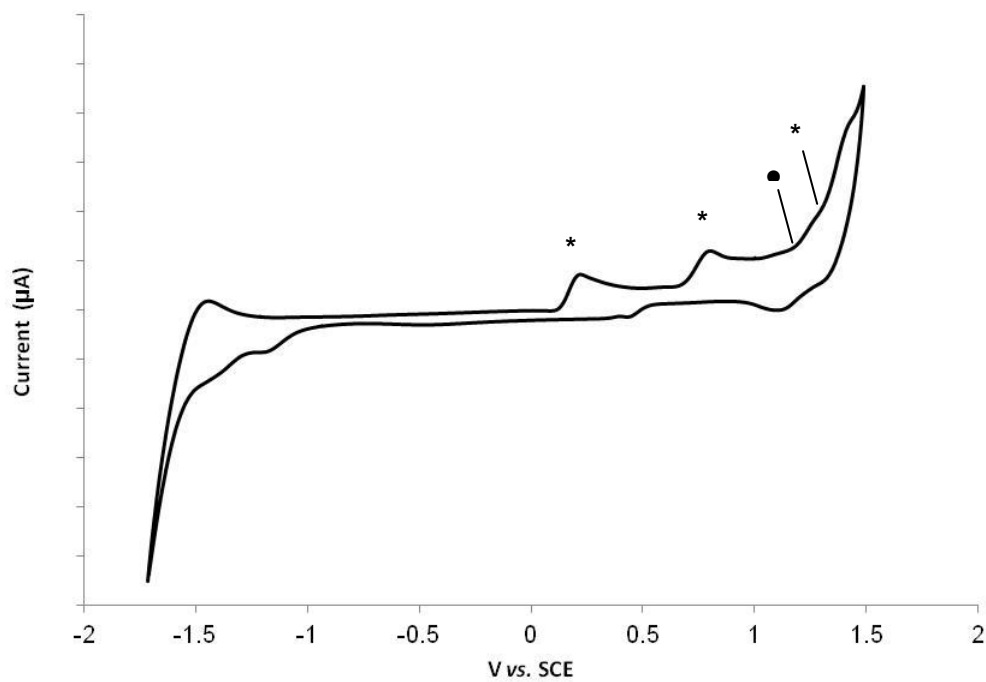


Fig. S2. Cyclic voltammogram of compounds **4** in the -1.8 V/1.6 V range, showing the Fe- and Ru-centered redox processes and another intense redox event (*). The second oxidation of the ZnTPP core is indicated by a dot (●). Conditions: CH₂Cl₂, 20 °C, [*n*-Bu₄N][PF₆] 0.1 M, scan rate: 0.1 V/s. Potential values given vs. SCE.

3. ^1H NMR Spectrum of $2[\text{PF}_6]_4$

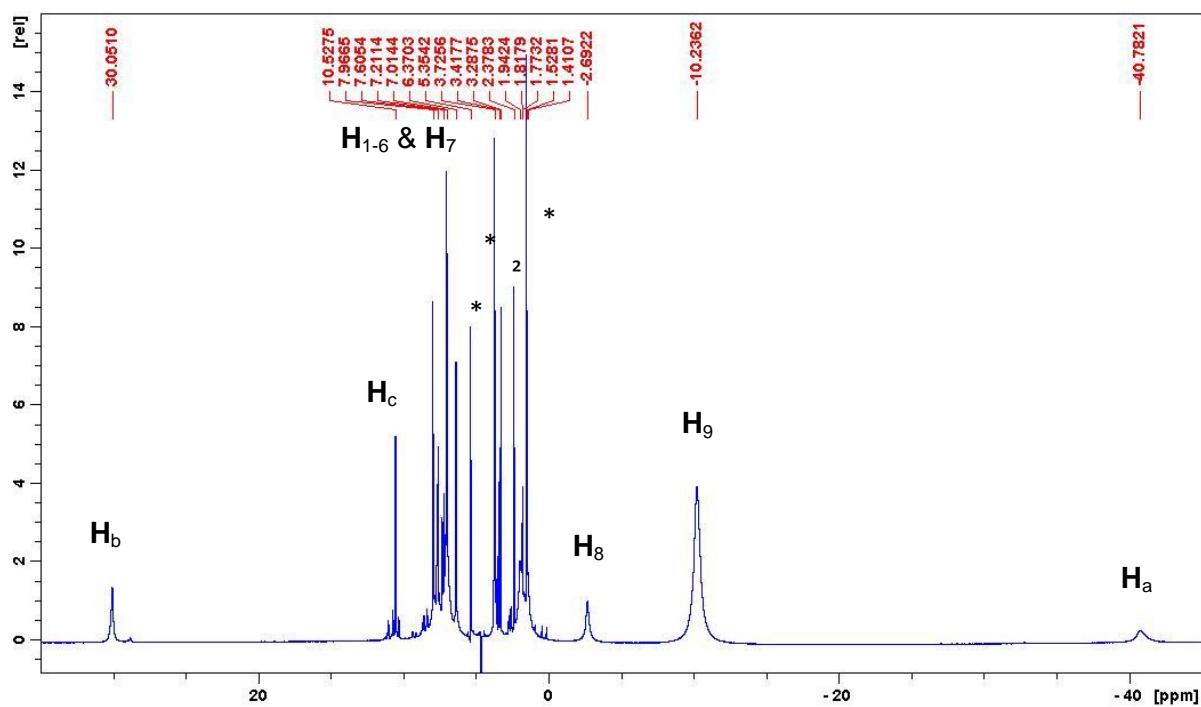


Fig. S3. ^1H NMR spectrum of $2[\text{PF}_6]_4$ in CD_2Cl_2 at 300 K. Numbering of selected protons according to Chart S1 (below). Signals corresponding to solvents are designated by asterisks (*).



Chart S1. ^1H nuclei numbering corresponding to the proposed assignment for $2[\text{PF}_6]_4$.

4. Spectroelectrochemistry of 3

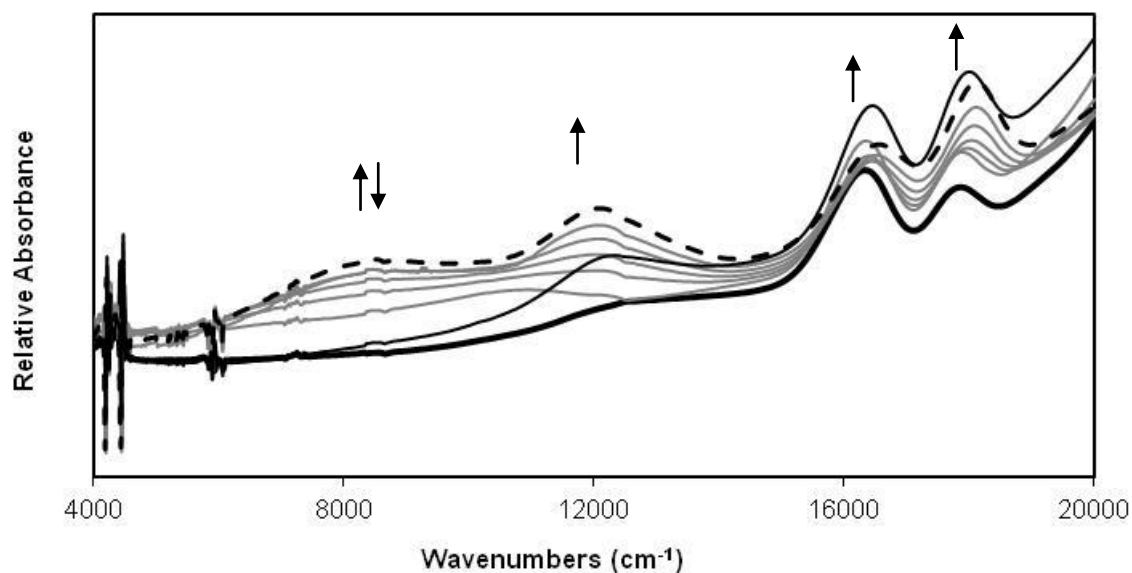


Fig. S4. Spectroelectrochemistry of compound **3**. The oxidized state is shown with a dotted line and the state recovered after back-reduction is given with a thin black line. Conditions: CH₂Cl₂, 20 °C, [*n*-Bu₄N][PF₆] 0.3 M, starting potential: -0.6 V, applied potential: 0.9 V vs. SCE. The region of the spectrum to higher energy of 20,000 cm⁻¹ is only marginally affected by redox changes.

5. Z-Scan Plots for 4

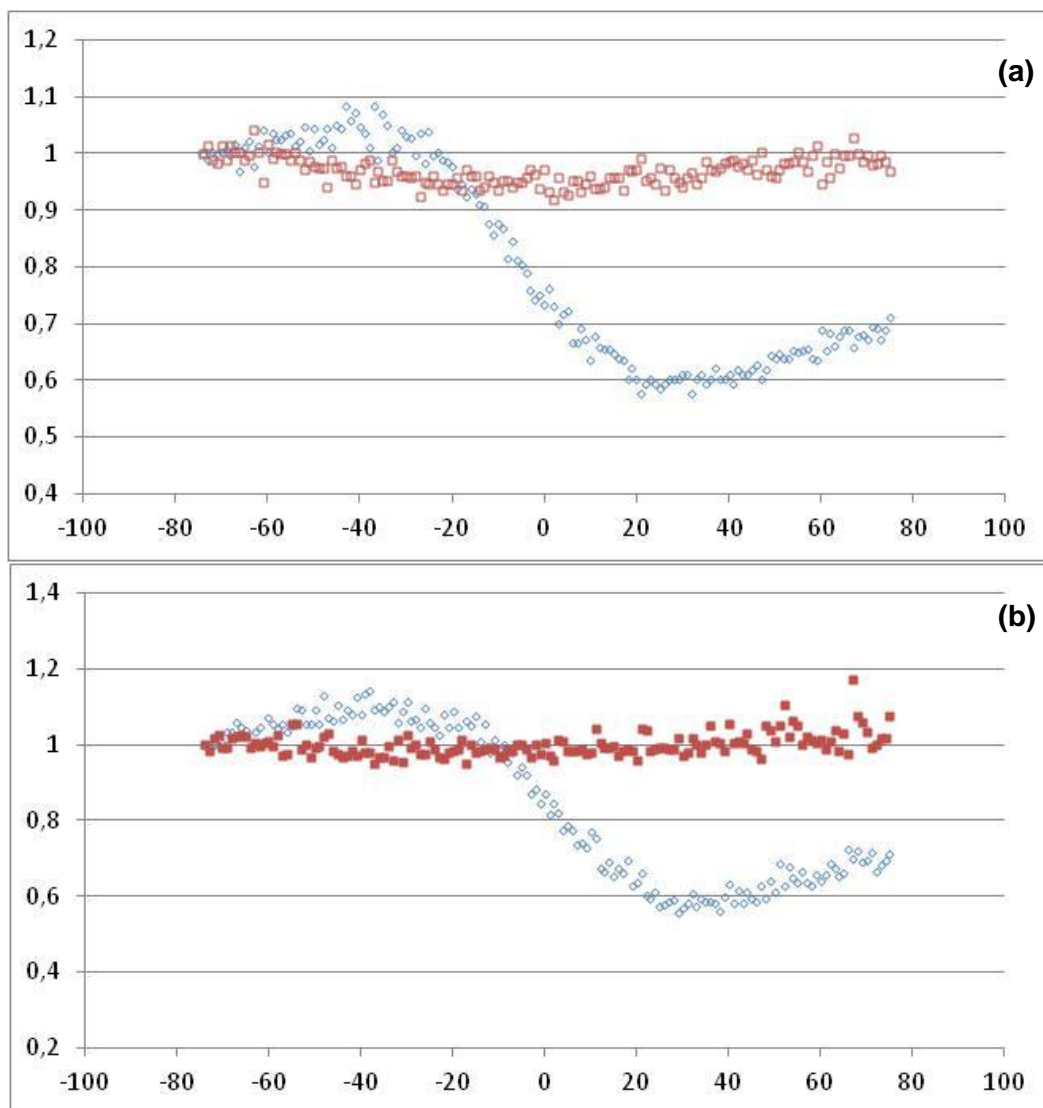


Fig. S4. Z-scan plots obtained for compound **4** at 560 nm (a) and 630 nm (b). Blue: closed-aperture traces. Red: open-aperture traces.